73

A potential role for spectrin during neurulation

T. W. SADLER, KEITH BURRIDGE AND J. YONKER

Department of Anatomy, 312 Swing Bldg, 217H, School of Medicine, University of North Carolina, Chapel Hill, North Carolina 27514, USA

SUMMARY

An actin–myosin complex located in apical regions of the neurectoderm has been postulated to play a role in neurulation. Numerous studies have documented the presence of microfilaments in this area and confirmed their composition as actin. By necessity, if such a contractile system is to exert a force, these filaments must be anchored in some way to the cell membrane. In this study, the presence of the actin-binding protein, spectrin (fodrin), is demonstrated in the neurectoderm of neurulating mouse embryos using antispectrin antibodies and indirect immunofluorescent techniques. The patterns of spectrin localization correlate with the previously reported regions of increased numbers of microfilaments and also with the morphology of the neural folds. Thus, during the initial stages of cranial fold elevation, a process reportedly dependent on increased glycosaminoglycan synthesis, little spectrin is present in the neuroepithelial cells. Later as the folds begin to converge toward the midline, deposition of the protein, as demonstrated by the intensity of fluorescence, is increased in the apices of these cells, and is most prominent in regions of greatest bending in the neural folds. Caudal neural fold regions show a similar pattern of staining. Thus, the hypothesis that a cytoskeletal system assists in neurulation is supported by these results, which for the first time demonstrate the presence of a putative actin–membrane attachment protein in a morphogenetically active system.

INTRODUCTION

An actin–myosin contractile system located in apical regions of the neurectoderm has been reported to play a role in the process of neurulation. Contraction of microfilament bundles presumably assists in the transformation of flattened sheets of neurectoderm cells of amphibians, chicks, and mammals into the neural tube. Evidence for this hypothesis is derived from (1) ultrastructural observations of neuroepithelial cells which demonstrate the presence of increased numbers of apical microfilaments during neurulation (Baker & Schroeder, 1967; Schroeder, 1973; Burnside, 1973; Karfunkel, 1974); (2) shape changes in ·the neurectoderm which show a narrowing of apical cell regions to create flask-shaped cells (Baker & Schroeder, 1967; Karfunkel, 1974; Schoenwolf & Franks, 1984); (3) binding of heavy meromyosin to apical microfilaments from chick neuroepithelia (Nagele & Lee, 1980); (4) localization of actin to apical regions of early chick embryo ectoderm (Wakely & Badley, 1982) and mouse neuroepithelial cells during neurulation (Sadler, Lessard, Greenberg & Coughlin, 1982) using anti-actin antibodies and indirect immunofluorescent techniques; (5) inhibition of

Key words: spectrin, neurulation, actin, cytoskeleton, antibody, mouse embryo.

neural tube closure following exposure of neurulating chick and mammalian embryos to cytochalasins (Lee & Kalmus, 1976; Wiley, 1980; Morriss-Kay, 1981).

Thus, the evidence suggests that in neuroepithelial cells a cytoskeletal network exists which acts as a force assisting in neurulation, presumably by contraction of the actomyosin complexes resulting in cell shape changes. By necessity this mechanism would require that the microfilament network be anchored to the plasma membrane. In this regard, several different mechanisms appear to exist for linking actin filaments to the plasma membranes of cells, although the molecular details for most of these systems have not been elucidated. The best characterized system is found in the mammalian erythrocyte where actin oligomers are linked to the higher molecular weight protein spectrin. Spectrin is associated with the protein ankyrin which, in turn, binds to the integral membrane protein band 3 (reviewed by Branton, Cohen & Tyler, 1981, and Goodman & Shiffer, 1983). During the last few years, a family of proteins related to erythrocyte spectrin have been identified in many cell types (Levine & Willard, 1981; Goodman, Zagon & Kulikowski, 1981; Repasky, Granger & Lazarides, 1982; Glenney, Glenney, Osborn & Weber, 1982a; Bennett, Davis & Fowler, 1982; Burridge, Kelly & Mangeat, 1982) including mouse blastocysts (Sobel & Alliegro, 1985). Similarly, a protein related to ankyrin has recently been found in non-erythrocyte tissue (Davis & Bennett, 1984). Although it is generally believed that a major function of non-erythrocyte spectrins is in the attachment of actin to the plasma membrane, other functions may also be important and the appropriateness of the erythrocyte as a model for the organization of spectrin in other cells has recently been questioned (Mangeat & Burridge, 1984). Whether non-erythrocyte spectrin has any role in morphogenetic movements has not been investigated. Therefore, since actin has been localized in the apical region of neuroepithelial cells undergoing morphogenetic movements (Sadler et al. 1982; Wakely & Badley, 1982) and has been implicated as generating these movements, the distribution of spectrin in these cells using antispectrin antibodies and indirect immunofluorescent techniques was investigated. Observations of spectrin localization were correlated with the shape changes of the neural folds and patterns of actin distribution previously described in these structures.

MATERIALS AND METHODS

The antibodies against brain spectrin (fodrin) used in this study have been described and characterized previously (Burridge et al. 1982). The specificity of the antibody with mouse embryonic tissue was checked by immunoblotting using a slight modification of the procedure of Towbin, Staehelin & Gordon (1979). Six 5- to 6-somite-stage embryos were homogenized and boiled in SDS–gel sample buffer (Laemmli, 1970). The sample was then electrophoresed on a 10 % SDS–polyacrylamide gel (Laemmli, 1970). Adjacent to the lane containing the mouse embryo sample, a sample of pig brain spectrin (fodrin) (Burridge et al. 1982) was electro-phoresed for comparative purposes. Following electrophoresis, the sample was transferred to a nitrocellulose sheet (Towbin et al. 1979) which was then incubated for 1 h in Tris-buffered saline (TBS) (150 mM-NaCl, 0·1 % NaN, 50 mM-Tris-Cl, pH 7·6) containing 3 % BSA, 0·2 % gelatin and 0·05 Tween-20. The nitrocellulose strip was then incubated for 90 min in a 1:1000 dilution of the rabbit anti-brain spectrin serum which was diluted in the above solution. After extensive

washing in TBS containing 0·2 % gelatin, and 0·05 % Tween-20, the strip was incubated with radio-iodinated, affinity-purified, goat anti-rabbit IgG for 1 h. After extensive washing the nitrocellulose strip was dried and exposed for autoradiography.

Mouse embryos of ICR strain were collected at various stages of neurulation (0–15 somites), and prepared for light microscopic observation or localization of antispectrin antibodies by indirect immunofluorescent techniques (IIF). For LM techniques, embryos were fixed for 0·5 h in modified Karnovsky's fixative (2 % glutaraldehyde, 2 % paraformaldehyde) in 0·1 M-cacodylate buffer, postfixed in 1 % OsO_4, dehydrated in a series of alcohols, and embedded in Araldite. One μm sections were then made through the cranial neural folds and stained with toluidine blue.

Embryos for IIF studies were fixed in Carnoy's fixative, dehydrated in 100 % ETOH, cleared in xylene, and embedded in paraffin. Sections from cranial and caudal neural tube regions were cut at 6 μm and rehydrated to phosphate-buffered saline (FAB, Difco). Sections were then covered with 30 μl of a solution of phosphate-buffered saline containing a 1:20 dilution of the antispectrin antibody. After 1 h, sections were washed in buffer and reacted for 1 h with fluorescein-conjugated goat antibody to rabbit immunoglobulin G (IgG) (Miles Laboratories). Control sections were stained with pre-immune IgG or with fractions adsorbed to columns of spectrin-coupled agarose.

RESULTS

Control slides for IIF consisted of reacting tissue sections with either pre-immune antisera or adsorbed antibody preparations. In both instances, only low levels of background tissue fluorescence were observed. As a second control, six 5- to 6-somite embryos were homogenized in SDS gel sample buffer, boiled, and run on 10 % polyacrylamide gels. The proteins in the gel were electrophoretically transferred to a nitrocellulose sheet which was immunoblotted with anti-brain spectrin (fodrin) followed by reaction with radio-iodinated second antibody, goat anti-rabbit IgG. The autoradiograph of the immunoblot revealed a major reactive band that co-migrated with the α-chain of brain spectrin (Fig. 1).

During early stages of neurulation (0–2 somites), cranial folds assume a bi-convex shape (Fig. 2). At this time, only a faint, incomplete fluorescence was observed and spectrin was localized to the apical regions of neuroepithelial cells along the neural groove. Cells located at the lateral edges of the cranial neural folds as well as spinal fold regions exhibited only a patchy, less-intense fluor-escence (Fig. 3). No staining was observed in basal regions of cranial neuro-epithelial cells.

At more advanced stages of neural tube closure, the intensity and amount of fluorescent staining increased. Thus, by the 4- to 5-somite stage, as the folds became more elevated and lost some of their convexity (Fig. 4), a fluorescent line was observed along the apical region of contiguous cranial neuroepithelial cells (Fig. 5). This staining pattern was maintained as the folds continued to elevate (Figs 6, 7) and remained during the process of fold convergence, which was initiated at the 7- to 8-somite stage (Figs 8, 9). By the 12-somite stage, the neural folds began to bend toward the midline (Fig. 10). At this stage, fluorescent staining was observed along the entire luminal surface of the neuroepithelium. However, the most intense staining was located at sites of greatest bending,

i.e. the lateral furrows (Fig. 11). This staining occurred along the apical surface of the cells and also extended between cells for a short distance (Figs 11, 12). Spinal folds exhibited a similar pattern as they converged toward the midline (Fig. 13). Overlying ectoderm failed to display fluorescence until the time of neural fold apposition. At this point, punctate localizations of fluorescence appeared in

Fig. 1. Immunoblot analysis of mouse embryos with anti-brain spectrin (fodrin). Six 5- to 6-somite embryos were boiled in SDS–gel sample buffer and electrophoresed in a 10 % polyacrylamide gel adjacent to a sample of pig brain spectrin (fodrin). Proteins were transferred from the gel onto nitrocellulose paper by electrophoresis. The figure shows the autoradiograph after reacting the nitrocellulose blot first with anti-spectrin, followed by radio-iodinated goat anti-rabbit antibodies. Lane 1 contained the sample of mouse embryos and lane 2 contained purified pig brain spectrin. In lane 2 a proteolytic fragment of spectrin at about 160×10^3 M_r is also detected by the antibody. Some staining is also seen at the dye front in the embryo sample.
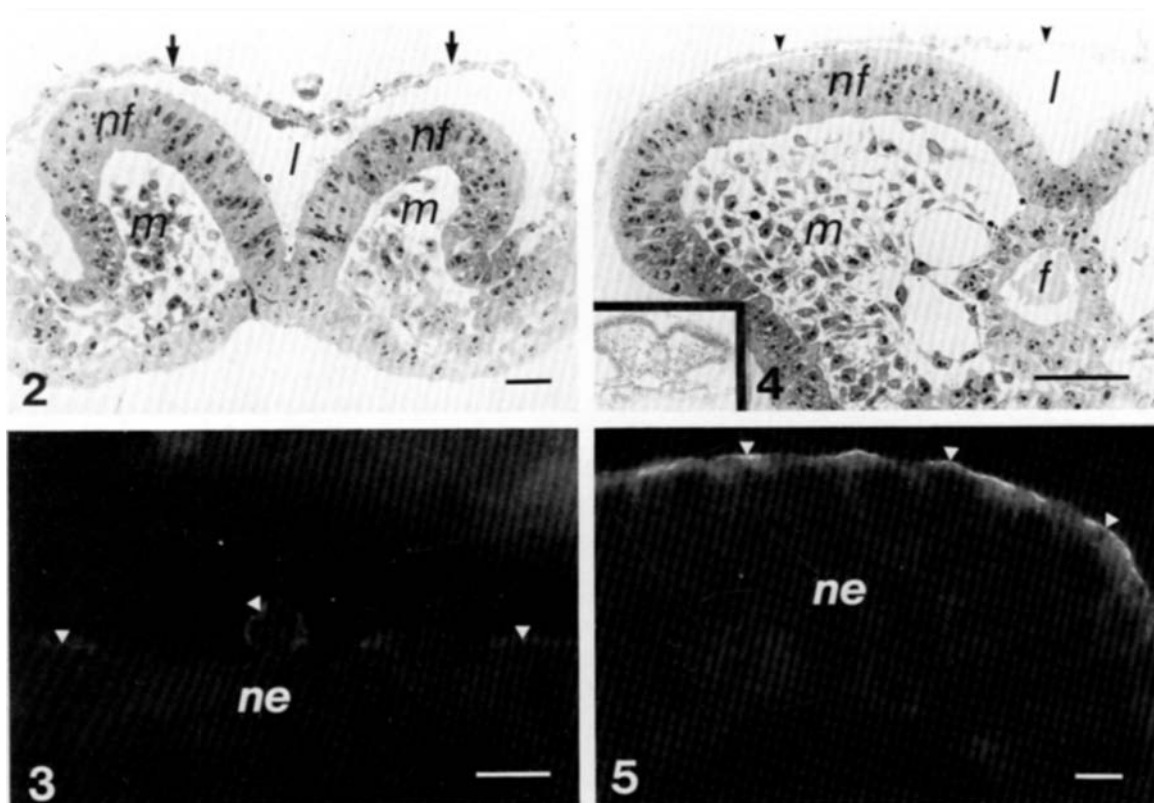
Fig. 2. Cross section through the headfold of 2-somite-stage mouse embryo. The neural folds (*nf*) have assumed a biconvex morphology and although they have elevated from the neural plate they have not yet begun to fold around the neural lumen (*l*). Mesenchyme (*m*); amnion (arrows). Toluidine blue. Bar, 25 μm.

Fig. 3. Fluorescent micrograph at high magnification showing the apices of neuro-epithelial cells (*ne*) located in the neural groove of a 2-somite-stage embryo. Only a faint incomplete fluorescence (arrowheads) is observed along the apical margin of these cells. Bar, 5 μm.

Fig. 4. Headfold (inset) region of a 4- to 5-somite-stage mouse embryo showing increased elevation and flattening of the neural folds (*nf*) preparatory to initiation of convergence around the neural lumen (*l*). Mesenchyme (*m*); foregut (*f*); amnion (arrowheads). Toluidine blue. Bar, 25 μm.

Fig. 5. Fluorescent micrograph of neuroepithelial cells (*ne*) from a 4- to 5-somite-stage embryo showing increased fluorescence along the apices (arrowheads) of the cells. The staining was continuous over all the neuroepithelial cells and consisted of intense patches at the apical border with lighter areas extending between cells. Bar, 5 μm.

apposing ectoderm cells which were responsible for making initial contact between the elevating neural folds.

DISCUSSION

During neurulation in the mouse, the neural plate is transformed from a flat sheet of neurectoderm cells into the neural tube, the forerunner of the central

nervous system. Included in this process is the formation of the neural folds which
lie on opposite sides of the neural groove. These folds become elevated, converge,
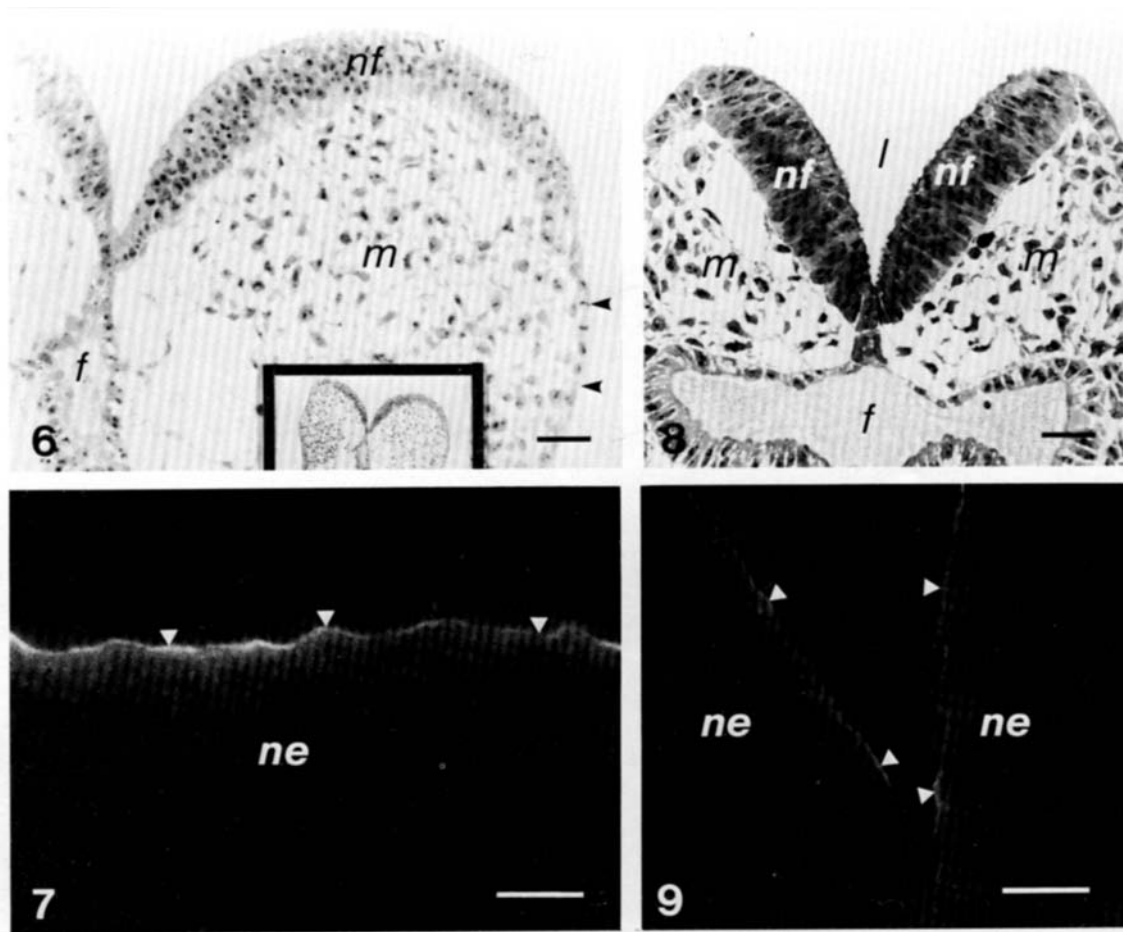and eventually fuse to form the tube-like structure. Although the tube is a

Fig. 6. Headfolds (inset) of a 5- to 6-somite-stage mouse embryo showing a continued
flattening of the neural folds (*nf*) and a thinning of the non-neural ectoderm
(arrowheads). By this stage, neural crest cells are completing their migration from the
neurectoderm–ectoderm junction and the neural folds will begin to converge.
Mesenchyme (*m*); foregut (*f*). Toluidine blue. Bar, 25 μm.

Fig. 7. Neuroepithelial cells (*ne*) showing intense fluorescence along their apical
borders (arrowheads) similar to the pattern observed at the 4- to 5-somite stage. Bar,
5 μm.

Fig. 8. Cross section through the hindbrain region of 7- to 8-somite-stage mouse
embryo demonstrating convergence of the neural folds (*nf*) around the neural lumen
(*l*). Mesenchyme (*m*); foregut (*f*). Toluidine blue. Bar, 25 μm.

Fig. 9. Fluorescent micrograph of the neuroepithelial cells (*ne*) deep within the neural
groove of a 7- to 8-somite-stage embryo. The apical pattern of fluorescence (arrow-
heads) is maintained and is present along the entire luminal surface of the cells. Bar,
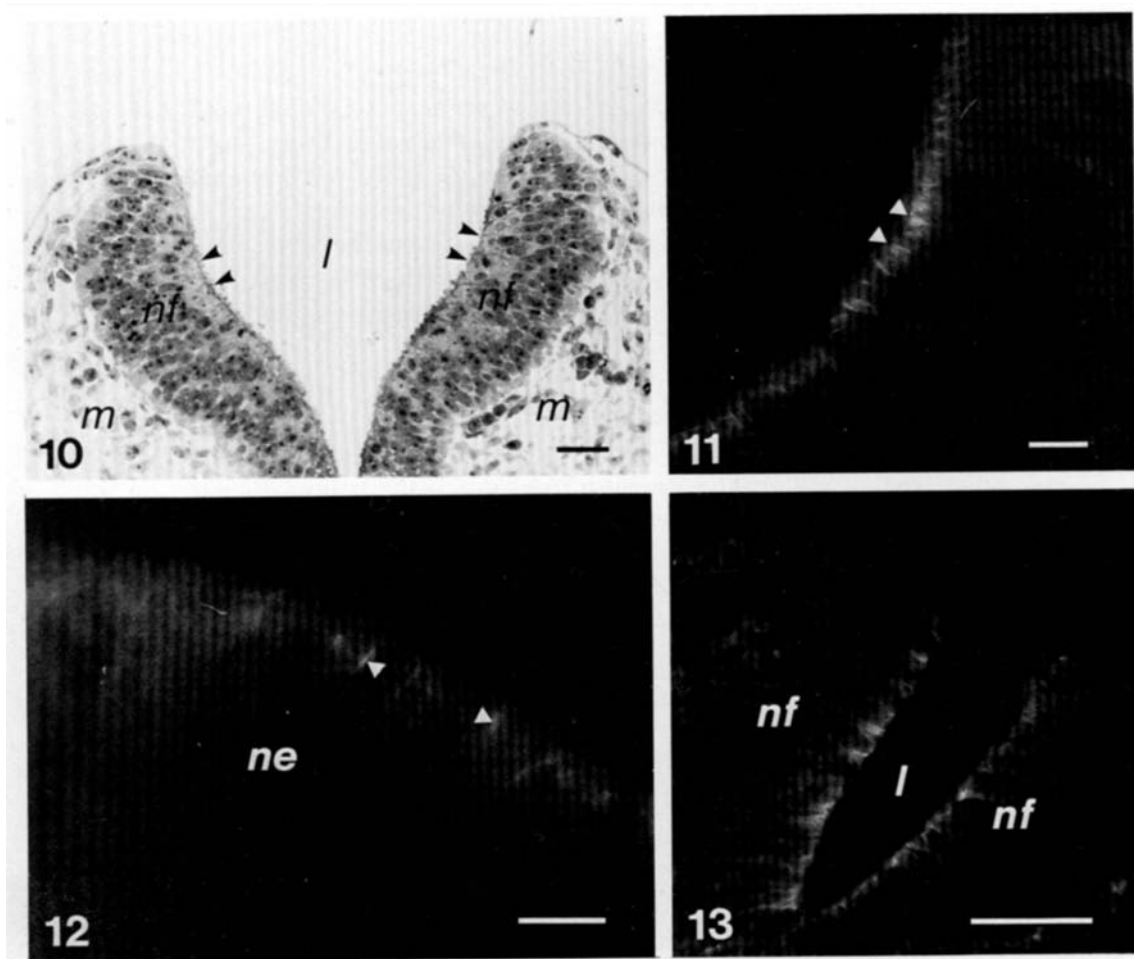5 μm.

Fig. 10. Transverse section through the hindbrain region of a 12-somite-stage mouse embryo at the time of lateral furrow (arrowheads) formation in the neural folds (*nf*). By this stage, the folds have reversed their biconvex shape and will soon meet in the midline and fuse. Also at this time neural crest cells migrate from the neurectoderm at the neurectoderm–ectoderm junction. Mesenchyme (*m*); neural lumen (*l*). Toluidine blue. Bar, 25 μm.

Fig. 11. Fluorescent micrograph of one neural fold from a 12-somite-stage embryo showing intense staining in the lateral furrow region (arrowheads). Also, the fluorescence extends between cells in their apices. Bar, 5 μm.

Fig. 12. Higher magnification of the neuroepithelial cells of a 12-somite-stage embryo showing fluorescence extending between apical cell borders (arrowheads). Bar, 5 μm.

Fig. 13. Fluorescent micrograph of a cross section through the spinal neural folds (*nf*) of a 15-somite-stage mouse embryo. The folds are close to fusion around the neural lumen (*l*) and the fluorescence pattern is similar to that observed in cranial neural folds at similar stages of development. Bar, 25 μm.

continuum, fold formation in the cranial region differs from that in spinal segments (Morriss-Kay, 1981). Thus, folds in the head region first assume a biconvex shape during which time the luminal surface of the neuroepithelial sheet is curved in the opposite direction from its eventual definitive form. From this point until approximately the 5-somite stage, the folds continue to elevate and gradually lose their convexity. Then, at the 5-somite stage, they flatten and by the 6- to 7-somite stage they begin to bend in the opposite direction around the future neural lumen. In contrast, spinal folds do not display the biconvex stage, but instead progress to convergence and fusion around the neural lumen, much as has been described in the chick (Schoenwolf, 1984).

The patterns of spectrin localization observed in the present study are consistent with the distribution of microfilaments during the morphogenetic process of neurulation (Baker & Schroeder, 1967; Burnside, 1973; Sadler *et al.* 1982). They are also consistent with shape changes occurring in the neural folds during this event. Initially, cranial folds assume a biconvex shape which appears to be effected by the synthesis of hyaluronic acid (Morriss & Solursh, 1978) and an increase in mesenchymal cell number (Morriss-Kay, 1981). At this stage, the distribution of microfilaments and spectrin in apical cell areas is sparse and restricted to the neural groove. Later as the folds reverse their shape and begin to converge, an increase in actin filaments and spectrin (as monitored by the distribution and intensity of fluorescence) occurs. Furthermore, this increase is restricted to the apical regions of the neurectoderm, which would be predicted by the contractile cytoskeletal model proposed for this event. During apposition of opposing neural folds in the region where the overlying ectoderm initiates contact, i.e. the hindbrain, increased deposits of spectrin are also observed. Again this pattern is consistent with the actin distribution pattern which showed an increased fluorescence in these cells at closure (Sadler *et al.* 1982). These ectoderm cells appear similar to fibroblasts in culture in that they extend numerous filopodia to make contact with and bridge the gap between opposing neural folds.

One difference between the localization of actin and spectrin occurred at the biconvex stage. At this point in development, actin, as demonstrated by IIF techniques, was localized in basal regions of neuroepithelial cells (Sadler *et al.* 1982) and it was suggested that microfilament contraction in this region might assist in the creation of the biconvex shape of the neural folds. In contrast, no localization of spectrin to this same region could be discerned. Whether spectrin is truly absent in this area or present at concentrations below the sensitivity of the technique employed is not known. The latter explanation appears likely, however, especially based on the low levels of spectrin detected using Western blot assays.

Additional evidence suggesting that spectrin is related to neural tube closure is derived by comparing localization of the protein in cranial *versus* spinal neural folds in embryos of different developmental stages. In young embryos (0–4 somites) undergoing initial stages of fold elevation, spectrin is concentrated in the neurectoderm of cranial neural folds and is not present in significant amounts in spinal regions. However, older embryos demonstrate the presence of the protein

in both cranial and caudal regions of the neuroepithelium. This distribution of spectrin coincides with the cephalocaudal direction of fold elevation and closure. Thus, cranial folds are the first to elevate followed shortly thereafter by spinal regions, with the entire process taking approximately 24–30 h (Morriss-Kay, 1981).

The localization of spectrin together with actin close to the apical plasma membrane of the folding neuroepithelial cells suggests that it has a role in the morphogenesis of the neural tube, presumably through attachment of actin filaments to the plasma membrane. It will be interesting to determine whether ankyrin or related proteins are similarly concentrated in the apical regions of these cells. It will also be important to determine whether perturbations of the spectrin distribution or function result in abnormal development. In this regard, defects in erythrocyte spectrin have been demonstrated in several patients with hereditary spherocytosis (Goodman *et al.* 1981). The defects prevent normal association of spectrin with actin and are presumed to be responsible for the membrane instability characteristic of this disorder. An equivalent defect in the spectrin of embryonic neuroepithelium would be expected to alter the normal morphology of this tissue which in turn could result in neural tube defects, such as spina bifida and exencephaly.

REFERENCES

BAKER, P. C. & SCHROEDER, T. E. (1967). Cytoplasmic filaments and morphogenetic movement in the amphibian neural tube. *Devl Biol.* **15**, 432–450.

BENNETT, V., DAVIS, J. & FOWLER, W. E. (1982). Brain spectrin, a membrane associated protein related in structure and function to erythrocyte spectrin. *Nature, Lond.* **299**, 126–131.

BRANTON, D., COHEN, C. & TYLER, J. (1981). Interaction of cytoskeletal proteins on the human red blood cell membrane. *Cell* **24**, 24–32.

BURNSIDE, B. (1973). Microtubules and microfilaments in amphibian neurulation. *Amer. Zool.* **13**, 989–1006.

BURRIDGE, K., KELLY, T. & MANGEAT, P. (1982). Nonerythrocyte spectrins: actin-membrane attachment proteins occurring in many cell types. *J. Cell Biol.* **95**, 478–486.

DAVIS, J. Q. & BENNETT, V. (1984). Brain ankyrin: a membrane-associated protein with binding sites for spectrin, tubulin, and the cytoplasmic domain of the erythrocyte anion channel. *J. biol. Chem.* **259**, 13 550–13 559.

GLENNEY, J. R., GLENNEY, P., OSBORN, M. & WEBER, K. (1982). An F-actin and calmodulin-binding protein from isolated intestinal brush borders has a morphology related to spectrin. *Cell* **28**, 843–854.

GOODMAN, R. D., ZAGON, I. S. & KULIKOWSKI, R. R. (1981). Identification of a spectrin-like protein in nonerythroid cells. *Proc. natn. Acad. Sci. U.S.A.* **78**, 7570–7574.

GOODMAN, S. R. & SHIFFER, K. (1983). The spectrin membrane skeleton of normal and abnormal human erythrocytes: a review. *Am. J. Physiol.* **244**, C121–C141.

KARFUNKEL, P. (1974). The mechanisms of neural tube formation. *Int. Rev. Cytol.* **38**, 245–271.

LAEMMLI, U. K. (1970). Cleavage of structural proteins during the assembly of the head of bacteriophage T4. *Nature, Lond.* **227**, 680–685.

LEE, H. Y. & KALMUS, G. W. (1976). Effects of cytochalasin B on the morphogenesis of explanted early chick embryos. *Growth* **40**, 153–162.

Levine, J. & Willard, M. (1981). Fodrin: axonally transported polypeptides associated with internal periphery of many cells. *J. Cell Biol.* **90**, 631–643.

Mangeat, P. & Burridge, K. (1984). Actin-membrane interaction in fibroblasts: What proteins are involved in this association? *J. Cell Biol.* **99**, 95s–103s.

Morriss-Kay, G. M. (1981). Growth and development of pattern in the cranial neural epithelium of rat embryos during neurulation. *J. Embryol. exp. Morph.* **65**, 225–241.

Morriss, G. M. & Solursh, M. (1978). Regional differences in mesenchymal cell morphology and glycosaminoglycans in early neural-fold stage rat embryos. *J. Embryol. exp. Morph.* **46**, 37–52.

Nagele, R. G. & Lee, H. Y. (1980). Studies on the mechanism of neurulation in the chick: Microfilament-mediated changes in cell shape during uplifting of neural folds. *J. exp. Zool.* **213**, 391–398.

Repasky, E. G., Granger, B. L. & Lazarides, E. (1982). Widespread occurrence of avian spectrin in non-erythroid cells. *Cell* **29**, 821–833.

Sadler, T. W., Lessard, J. L., Greenberg, D. & Coughlin, P. (1982). Actin distribution patterns in the mouse neural tube during neurulation. *Science* **215**, 172–174.

Schoenwolf, G. C. (1984). On the morphogenesis of the early rudiments of the developing central nervous system. *Scanning Electron Microsc.* **1**, 289–308.

Schoenwolf, G. C. & Franks, M. V. (1984). Quantitative analyses of changes in cell shapes during bending of the avian neural plate. *Devl Biol.* **105**, 257–272.

Schroeder, T. E. (1973). Cell constriction: Contractile role of microfilaments in division and development. *Amer. Zool.* **13**, 949–960.

Sobel, J. S. & Alliegro, M. A. (1985). Changes in the distribution of a spectrin-like protein during development of the preimplantation mouse embryo. *J. Cell Biol.* **100**, 333–336.

Towbin, H., Staehelin, T. & Gordon, J. (1979). Electrophoretic transfer of proteins from polyacrylamide gels to nitrocellulose sheets; procedure and some applications. *Proc. natn. Acad. Sci. U.S.A.* **76**, 4350–4354.

Wakely, J. & Badley, R. A. (1982). Organization of actin filaments in early chick embryo ectoderm: an ultrastructural and immunocytochemical study. *J. Embryol. exp. Morph.* **69**, 169–182.

Wiley, M. J. (1980). The effects of cytochalasins on the ultrastructure of neurulating hamster embryos *in vivo*. *Teratology* **22**, 59–69.